



## Molecular Crystals and Liquid Crystals Science and Technology. Section A. Molecular Crystals and Liquid Crystals

Publication details, including instructions for authors and subscription information:

<http://www.tandfonline.com/loi/gmcl19>

## Light Scattering and Photon Correlation Spectroscopy of Filled and Confined Liquid Crystals

Fouad Aliev<sup>a</sup>, Markus Kreuzer<sup>b</sup>, Nelson Tabiryan<sup>c</sup>  
& Boris Zel'dovich<sup>c</sup>

<sup>a</sup> Department of Physics, University of Puerto Rico,  
San Juan, PR, 00931, USA

<sup>b</sup> IAP, Darmstadt University of Technology, 64289,  
Darmstadt, Germany

<sup>c</sup> CREOL, University of Central Florida, Orlando, FL,  
32816, USA

Version of record first published: 24 Sep 2006

To cite this article: Fouad Aliev, Markus Kreuzer, Nelson Tabiryan & Boris Zel'dovich (1998): Light Scattering and Photon Correlation Spectroscopy of Filled and Confined Liquid Crystals, *Molecular Crystals and Liquid Crystals Science and Technology. Section A. Molecular Crystals and Liquid Crystals*, 320:1, 173-191

To link to this article: <http://dx.doi.org/10.1080/10587259808024394>

Full terms and conditions of use: <http://www.tandfonline.com/page/terms-and-conditions>

This article may be used for research, teaching, and private study purposes. Any substantial or systematic reproduction, redistribution, reselling, loan, sub-licensing, systematic supply, or distribution in any form to anyone is expressly forbidden.

The publisher does not give any warranty express or implied or make any representation that the contents will be complete or accurate or up to date. The accuracy of any instructions, formulae, and drug doses should be independently verified with primary sources. The publisher shall not be liable for any loss, actions, claims, proceedings, demand, or costs or damages whatsoever or howsoever caused arising directly or indirectly in connection with or arising out of the use of this material.

## Light Scattering and Photon Correlation Spectroscopy of Filled and Confined Liquid Crystals

FOUAD ALIEV<sup>a</sup>, MARKUS KREUZER<sup>b</sup>, NELSON TABIRYAN<sup>c</sup>, AND BORIS ZEL'DOVICH<sup>c</sup>

<sup>a</sup>Department of Physics, University of Puerto Rico, San Juan, PR 00931, USA, <sup>b</sup>IAP, Darmstadt University of Technology, 64289 Darmstadt, Germany, <sup>c</sup>CREOL, University of Central Florida, Orlando, FL 32816, USA

We present the results of photon correlation spectroscopy investigations of the influence of the confinement and interfaces on the behavior of nematic liquid crystals (NLC) filled with aerosil particles as well as dispersed in porous matrices of different pore geometry and size. The experiments show significant changes in physical properties of LC in such confinements and suggest that there is some evidence for glass-like dynamical behavior, although bulk LC do not have glassy properties. In NLC with nanoparticle network, at least two well identified decays were observed. We attribute the first decay to the director fluctuations of the bulk NLC. The second, glass-like decay, could be related to director dynamics in surface layers at aerosil - LC interface. The mode corresponding to motions of individual aerosil nanoparticles was not detected. This confirms that the aerosil particles form a network in the LC.

Keywords: liquid crystals; confinement; dynamical behavior

## INTRODUCTION

Liquid crystals (LC) dispersed in polymer matrices (PDLC)<sup>[1]</sup> and in inorganic porous matrices<sup>[2]</sup> are materials extremely important for both applications and for fundamental physics of confined systems. This stimulates intensive research of polymer dispersed and confined LC<sup>[3–5]</sup>. A variety of new properties and phenomena such as a modification of phase transitions, orientational order, elastic properties, director field, and some aspects of

dynamical behavior<sup>[6-10]</sup> has been studied both experimentally and theoretically for LC confined in random porous networks and cylindrical pores. Searches for new materials for electrooptic devices and particularly for displays has led to the creation of a new material - filled nematics (FN)<sup>[11-13]</sup>. This materials are stable dispersions of inorganic particles formed by the aggregation of amorphous silica spheres with diameters in the range of ten nanometers. Agglomeration of the chain-like aggregates forms a three-dimensional network dividing the liquid crystal into LC domains building a system of randomly orientated capillaries filled with nematic liquid crystal.

Although great success in the understanding of the physical properties of liquid crystals confined in porous media with different size, shape of pores and different structure of porous matrix was achieved, little work has been done to characterize the influence of confinement on different aspects of dynamical behavior of confined LC.

In this paper we present the results photon correlation spectroscopy investigations, complemented with static light scattering experiments, of the influence of the confinement and interfaces on the behavior of NLC in both physical situations: filled with aerosil particles as well as dispersed in porous matrices of different pore geometry and size. These systems are anisotropic (at least at short spatial scales) and heterogeneous materials characterized by a very developed interface. Investigations of LC in cylindrical pores together with studies in random porous matrices and filled LC, makes it possible to separate the role of random structure and domain formation from the contributions due to existence of LC - solid interfaces and pure finite size effect in relaxation of order parameter or director fluctuations. The experiments show significant changes in physical properties of confined and filled NLC (FN), and provide some evidence for glass-like dynamical behavior, although bulk liquid crystal does not have glassy properties neither in anisotropic nor in isotropic phases.

## EXPERIMENTAL

We performed photon correlation measurements using a  $\lambda = 0.6328 \mu\text{m}$  He-Ne laser and the ALV-5000/Fast Digital Multiple Tau Correlator (real time) operating over delay times from 12.5 ns up to  $10^3$  s with the Thorn EMI 9130/100B03 photomultiplier and the ALV preamplifier. In addition, we used ALV/LSE unit which allows, simultaneously with photon correlation measurements, monitoring of the laser beam intensity and stability of its space position as well as monitoring of the intensity of scattered light integrated over all frequencies (static light scattering).

The depolarized component of scattered light was investigated. In the isotropic phase of bulk LCs, observation of the depolarized component of the scattered light makes it possible to detect the contribution connected with order parameter fluctuations only. It also allows to exclude the scattering from the porous matrix when LC is in pores, or from the network structure in the case of FN.

In the dynamic light scattering experiment, one measures the intensity-intensity autocorrelation function

$$g_2(t) = \langle I(t)I(0) \rangle / \langle I(0) \rangle^2. \quad (1)$$

The intensity-intensity autocorrelation function  $g_2(t)$  is related to the dynamic structure factor  $f(q,t)$  of the sample by

$$g_2(t) = 1 + kf^2(q,t), \quad (2)$$

where  $k$  is a contrast factor that determines the signal-to-noise ratio and  $q = 4\pi n \sin(\Theta/2)/\lambda$ , ( $n$  is the refractive index,  $\Theta$  - the scattering angle and  $\lambda$  is the wavelength of laser radiation). We found that the intensity-intensity autocorrelation functions were  $q$ -independent for 5CB in porous glasses, and almost  $q$ -independent for 5CB in cylindrical pores. All dynamic light scattering data that we discuss below for LC confined in porous matrices were obtained at  $\Theta=30^\circ$ .

We used matrices with randomly oriented, interconnected pores (porous glasses with average pore sizes of 10 nm and 100 nm) and parallel cylindrical pores (Anopore membranes with pore diameters of 20 nm and 200 nm).

The glass plates with the size of the pores 10 nm have dimensions  $1\text{cm} \times 1\text{cm} \times 0.2\text{cm}$ . All surfaces of these matrices were optically polished. Since the linear size of optical inhomogeneities as determined by the pore size is much smaller than the wavelength of visible light, this sample was optically transparent. In the case of 100 nm pore matrices, which are opaque, the thickness of the samples was chosen to be 0.2 mm to reduce the contribution from multiple scattering. Anopore membranes had thickness of 60  $\mu\text{m}$ .

The FN we have used had concentration of silica particles in NLC E48 2.8 % of the volume. For investigations of Filled LC, we prepared a layer of material between two glass substrates the surfaces of which were not treated, and no particular orientation was enforced by the boundaries. The thickness of the sample was 60  $\mu\text{m}$  to avoid multiple scattering.

## STATIC LIGHT SCATTERING IN CONFINED 5CB

From static light scattering experiments we obtained that the temperature of the nematic - isotropic phase transition in 100 nm random pores, 20 nm and 200 nm cylindrical pores is depressed compared to that in the bulk NLC, the transition is not as sharp as in the bulk LC, it is smeared out and occupies finite temperature region. The temperature dependencies of the intensity of scattered light ( $I_{sc}$ ) for 5CB in 20 nm and 200 nm cylindrical pores are presented in Fig. 1.

For 5CB confined in 10 nm random pores we found that there is no well defined phase transition from ordered phase to the phase in which long range order is completely absent, or opposite from disordered phase to the phase with perfect long range orientational order. And for filled

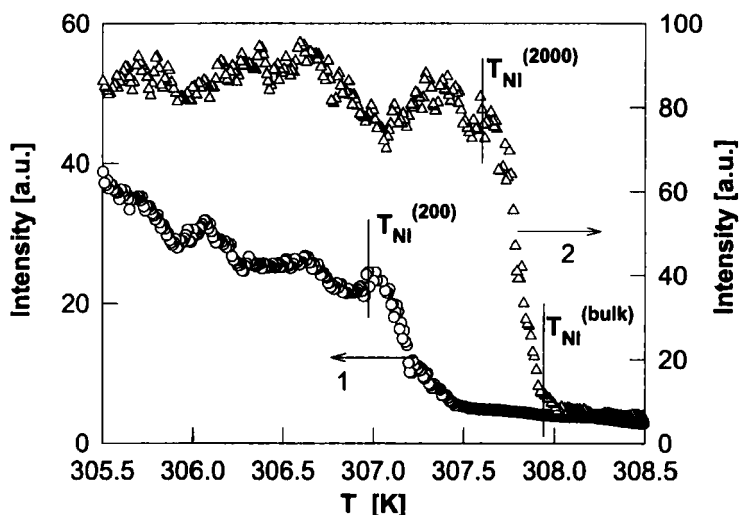


FIGURE 1 Temperature dependence of the intensity of scattered light for 5CB in cylindrical pores: (1) - 200 Å (2) - 2000 Å.

LC, in static light scattering experiments, we have not observed noticeable changes compared to the bulk behavior of E48. The temperature dependence of  $I_{sc}$  in the isotropic phase of confined LC is different from that in the bulk. In pores  $I_{sc}$  is almost independent of temperature (Fig. 1) in the temperature range corresponding to the isotropic phase. In the bulk isotropic phase this intensity is temperature dependent and exhibits the mean-field theory critical exponent expected near a second-order transition at a temperature  $T^*$  preempted by a first order phase transition at  $T_{NI}$ , namely:  $I_{sc} \sim 1/(T - T^*)$ .

The difficulty in determination of the phase transition temperature in finite systems, the difficulty is that the transition region occupies a finite temperature interval and it is unclear what should be regarded as the transition temperature. The combination of static and dynamic light scattering methods is very useful to determine the phase transition temperature of LC in pores. In dynamic light scattering experiment, only one relaxational process due to fluctuations of the order parameter should be

observed in isotropic phase. In the nematic phase, the decay of  $g_2(t)$  is due to director fluctuations. The difference in relaxation times of these two processes is of three orders of magnitude, and it is very easy to identify the nature of the relaxational process and the corresponding phase state of the LC. We determine the nematic-isotropic phase transition temperature for LC in pores as a temperature below which there is no visible decay due to order parameter fluctuations. These temperatures coincide with the temperatures at which the rise in the intensity of the scattered light (when temperature is decreased) saturates (see curves 1 and 2 in Fig. 1). We found thus the following values of the nematic - isotropic phase transition temperatures for 5CB in pores: 307.5 K (100 nm random pores), 307.6 K (200 nm cylindrical pores) and 307.0 K (20 nm cylindrical pores).

## CONFINED LIQUID CRYSTALS

The spatial confinement has a strong influence on the dynamic properties of LC investigated in photon correlation experiments. A slow relaxational process which does not exist in the bulk phase appears in both confined and filled LC. The difference between the dynamic behavior of bulk multidomain NLC 5CB and E48, and 5CB confined in random as well as in cylindrical pores can be seen by comparison of autocorrelation functions presented in Fig. 2. and Fig. 3. The Dynamic light scattering in bulk NLC is very well understood<sup>[10]</sup>, and the main contribution to the intensity of scattered light is due to the director fluctuations. In a uniformly oriented nematic sample, there are two modes determined by these fluctuations. The first mode is determined by a single combination of splay and bend distortions and the second mode by a combination of twist and bend distortions, and each of these modes is described by single exponential decay function. If for simplicity we assume that all six Leslie coefficients have the same order of magnitude  $\sim \eta$  ( $\eta$  is an average viscosity), and the three elastic constants (bend, splay and twist) are equal ( $K$ ) then the relaxation



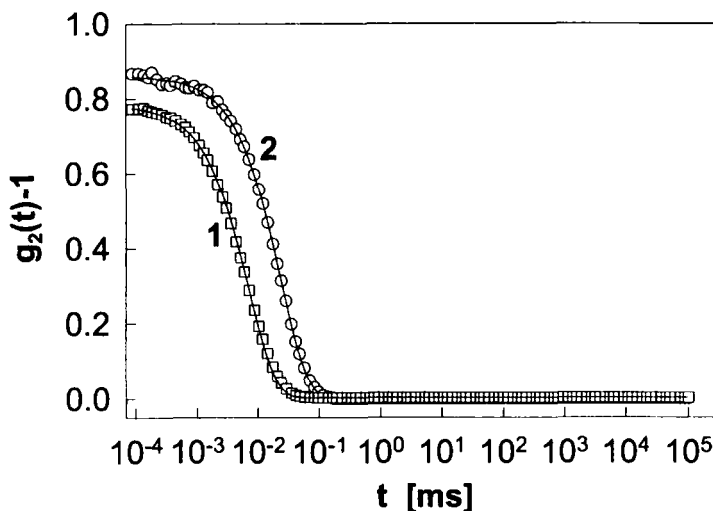


FIGURE 2 Intensity/intensity autocorrelation functions for 5CB: (1) - bulk 5CB,  $T=306.2$  K and (2) - bulk E48,  $T=359.5$  K Open circles correspond to the experimental data, solid lines are the result of fitting.

time of director fluctuations is

$$\tau = \eta / K q^2 \quad (3)$$

and has the same order of magnitude  $\sim 10^{-5}$  s for the both modes. The corresponding decay function is an exponential decay function:

$$f(q, t) = a \cdot \exp(-t/\tau). \quad (4)$$

The autocorrelation functions obtained for both 5CB and E48 in multidomain bulk nematic phase are perfectly described by the decay function (4) as it is shown in Fig. 2. The relaxation time  $\tau = 1.4 \cdot 10^{-5}$  s which corresponds to bulk 5CB - the curve 1 (Fig. 2) and  $\tau = 2.4 \cdot 10^{-5}$  s - bulk E48, the curve 2, are in agreement with the theory<sup>[14]</sup>. It is clear from Fig. 3 that the relaxation processes in 5CB confined in the matrices with random and cylindrical pores are essentially nonexponential, as it is usually observed in glasses and glass-like systems<sup>[15]</sup>. The long time tail of the relaxation process for 5CB in pores can not be described by using the

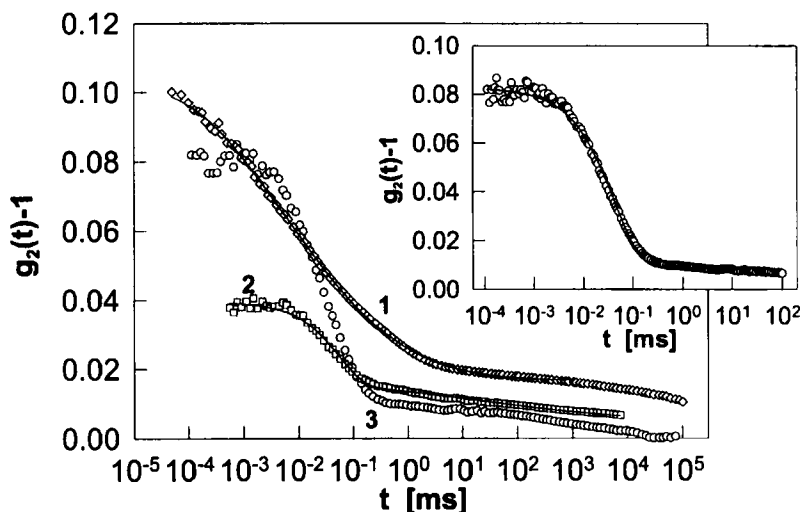


FIGURE 3 Intensity/intensity autocorrelation functions for 5CB: (1) - in 10 nm random pores,  $T=295.8$  K; (2) - in 20 nm cylindrical pores,  $T=306.9$  K, (3) - in 200 nm cylindrical pores at  $T = 307.3$  K. The inset shows the result of fitting for 5CB in 200 nm pores. Open symbols are the experimental data, solid lines - fitting.

standard form of the dynamical scaling variable  $(t/\tau)$  and the decay function cannot be reduced to a superposition of finite number of exponential terms.

For so slow dynamics and such a wide spectrum, it is reasonable to use the ideas<sup>[6,16,17]</sup> of activated dynamical scaling with the scaling variable  $x = \ln t / \ln \tau$ . We are not able to find the correlation function (or a superposition of correlation functions) which would satisfactorily and quantitatively describe the whole experimental data from  $t = 10^{-4}$  ms up to  $t = 10^6$  ms. However we found that in the time interval  $10^{-3}$  ms –  $10^3$  ms (6 decades on the time scale) the decay function

$$f(q, t) = a \cdot \exp(-(t/\tau_1)^\beta) + (1 - a) \cdot \exp(-x^z), \quad (5)$$

where  $x = \ln(t/\tau_0)/\ln(\tau_2/\tau_0)$  and  $\tau_0 = 10^{-8}$  s provides suitable fitting for 5CB in narrow (10 nm and 20 nm) pores. In the second term of

Eq. (5),  $z = 3$  corresponds to the activated scaling theory for random-field systems with conserved order parameter<sup>[16]</sup> (which is not our case since LC are the systems with non conserved order parameter). In the theory<sup>[17]</sup> for  $d$ -dimensional short-range Ising spin-glasses,  $z$  is determined by the dimensionality of the system:  $z = d/(d - 1)$ , and the correlation function corresponding to the second term in Eq. (5) describes slow relaxation of large isolated clusters above the spin-glass transition.

For 5CB in 10 nm random pores the second term in relationship (5) dominates, whereas for 20 nm pores the contribution from the first term is much more visible. The fitting parameters corresponding to curves (1) and (2) in Fig. 2 are: (1) -  $z=2.3$ ,  $\tau_2=0.04$  ms (exponential decay is neglected); (2) -  $\tau_1 = 0.07$  ms,  $z = 3.6$ ,  $\tau_2 = 3$  s.

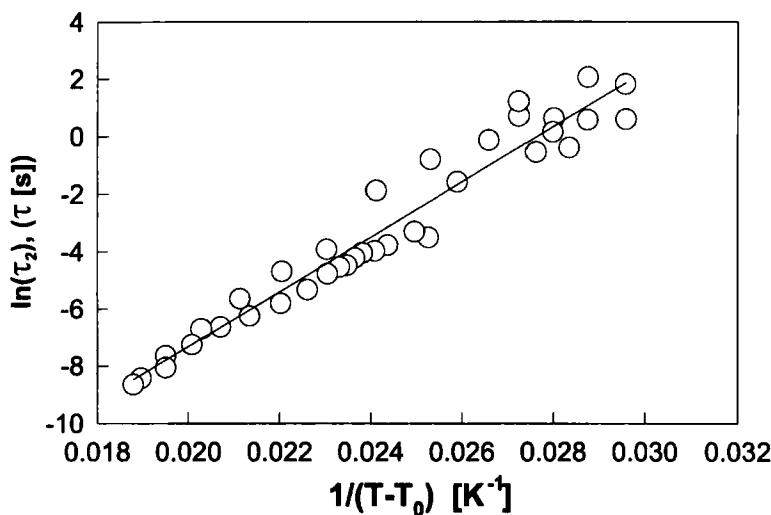


FIGURE 4 The relaxation time as a function of the inverse temperature for 5CB in 10 nm random pores.

The relaxation time of the slow process for 5CB in 10 nm pores strongly increases, as shown in Fig. 4, when the temperature decreases from 300 K up to 270 K varying from  $1.7 \times 10^{-4}$  s to 14 s in this tempera-

ture range. The data analysis shows that the temperature dependence of the relaxation times for 5CB in 100 nm random pores, in the temperature interval (270-300) K, follows the Vogel-Fulcher law<sup>[15]</sup>

$$\tau = \tau_0 \exp(B/(T - T_0)) \quad (6)$$

with parameters:  $\tau_0 = 1.4 \cdot 10^{-11} \text{ s}$ ,  $B = 847 \text{ K}$  and  $T_0 = 246 \text{ K}$ .

The dynamical behavior of 5CB confined in large pores (100 nm and 200 nm) was closer to the bulk behavior, and bulk-like relaxation of director fluctuations is observed. But in pores this relaxation is a stretched exponential which is typical for glass forming systems. The first term in the Eq. (5) adequately describes the experimental data up to  $t < 0.1 \text{ s}$ .

The data presented in the inset of Fig. 3 have parameters  $\tau = 0.1 \text{ ms}$  and  $\beta = 0.8$ . Detailed data analysis shows that in 10 nm pores, at temperatures above  $\simeq 300 \text{ K}$  the relaxation process separates into two processes, and this separation become more clear with further temperature rise. In 100 Å pores slow relaxational processes exist even at temperatures corresponding to the bulk isotropic phase, but the first (fast) process dominates. We attribute the first (fast) decay in 100 Å pores which is clearly seen at  $T > 301 \text{ K}$  to the fluctuations of the order parameter. This decay dominates at high temperatures. The amplitude of the slow decay, which dominates at low temperatures decreases with increasing temperature and is almost independent on temperature, at temperatures corresponding to the bulk isotropic phase.

In 100 nm pores, we observed two decays only at temperatures below nematic-isotropic phase transition temperature in pores. A typical autocorrelation function for 5CB confined in 100 nm and its comparison with data for filled LC are presented in the next section.

We would like to note that though the first decay weakly depends of temperature, the decay immediately vanishes when the LC is in its isotropic phase. The slow decay also vanishes at temperatures corresponding to isotropic phase in 100 nm random pores, 20 nm and 200 nm cylindrical pores, and a very fast decay, typical for the order parameter in the

bulk isotropic phase appears, with relaxation time  $\tau \sim 10^{-7}$  s. Thus the slow decay in both pores is connected with the existence of nematic (or nematic like in 10 nm pores) ordering. Since in 10 nm pores nematic ordering exists even at sufficiently high temperatures, the slow decay also exists at temperatures corresponding to the bulk isotropic phase.

One of the possible explanations (together with the model suggested in<sup>[6,7]</sup> and the model based on slow motions of domains<sup>[8]</sup> of the origin of the slow decay may be a formation of interfacial layers on the pore wall. The thickness (that means also the volume fraction) of these layers should be temperature dependent and archives its minimum magnitude in isotropic phase. The minimum thickness may be equal to the thickness of monolayer. In 100 nm pores the volume fraction of first layer formed on the pore wall is very small and therefore is not detected in the dynamic light scattering experiment in the temperature range corresponding to the isotropic phase.

## FILLED NEMATICS

Filled Nematics are suspensions of highly dispersed silica in the nematic phase of liquid crystal. The pyrogenic silica – that is obtained by hydrolysis of silicon tetrachloride in an oxygen-hydrogen flame – can form densely packed stable suspensions in which the silica occupies only 2 to 3 percent of the volume. The spherical primary particles of amorphous silicon dioxide obtainable with average diameters between 7 and 16 nm (Aerosil from Degussa<sup>[18]</sup>) form aggregates of irregularly branched strings via  $\equiv\text{Si}-\text{O}-\text{Si}\equiv$  moieties. The  $\equiv\text{SiOH}$  groups on the surface of these aggregates form hydrogen bonds between different particles leading to the formation of agglomerates.

Investigations have shown that the agglomeration of 2-3 volume percent of Aerosil particles in a nematic phase of liquid crystal forms a three-dimensional network dividing the liquid crystal into LC domains with a

linear size of approximately  $2500 \text{ \AA}$  <sup>[13]</sup>. For most purposes the system can be simplified and described as a system of randomly orientated capillaries filled with nematic liquid crystal<sup>[19]</sup>. From this point of view the dynamical properties of filled nematics should have some similarities with properties of LC confined in  $1000 \text{ \AA}$  random porous matrices. Both of them have disordered structure and highly developed solid-liquid crystal interface (typically  $300 \text{ m}^2$  per gram dispersed silica in filled nematics). However, assuming strong anchoring of the nematic director at the surfaces of the particles forming the skeleton<sup>[12,20]</sup>, not only the surfaces act elastically on the director, but the director also acts on the surfaces *and thus on the particles*. This flexibility of the framework and its temperature dependence may bring new phenomena and new properties absent in systems based on rigid matrices.

The main difference between structure of LC confined in porous matrices and filled LC is as follows. Porous glass matrices or Anopore membranes have solid network the structure of which is temperature independent. The particles in FN are capable of changing their mutual arrangement<sup>[13]</sup> and the network structure in the case of FN. According to the picture given in<sup>[13]</sup>, the network formation (aerosil frame) is accompanied by formation of LC domains with linear size about  $250 \text{ nm}$  with random distribution of director orientation of each domain. From this point of view, the dynamical properties of filled LC should have some similarities with properties of LC confined in  $100 \text{ nm}$  random porous matrices. However the flexibility of the framework of filled LC may introduce new properties absent in systems based on rigid matrices.

We observed a glass-like non-exponential relaxational process also in filled LC. We obtained that the temperature dependencies of relaxational processes characterized by  $g_2(t)$  in filled LC in the temperature range  $274\text{K} < T < 340\text{K}$  are very different from that in the range  $340\text{K} < T < 360\text{K}$ . The intensity/intensity autocorrelation functions of filled LC are different from  $g_2(t)$  observed for bulk LC in the both temperature regions. These functions are not single exponential but are described

by superposition of at least two functions. Moreover, at temperatures  $T > 340\text{K}$ , a presence of an additional slow decay in the time range  $t > 10\text{ ms}$  is obvious without detailed analysis.

The autocorrelation function typical for temperatures  $T < 340\text{K}$  is presented in the Fig. 5. It is clear that the experimental data (circles) can

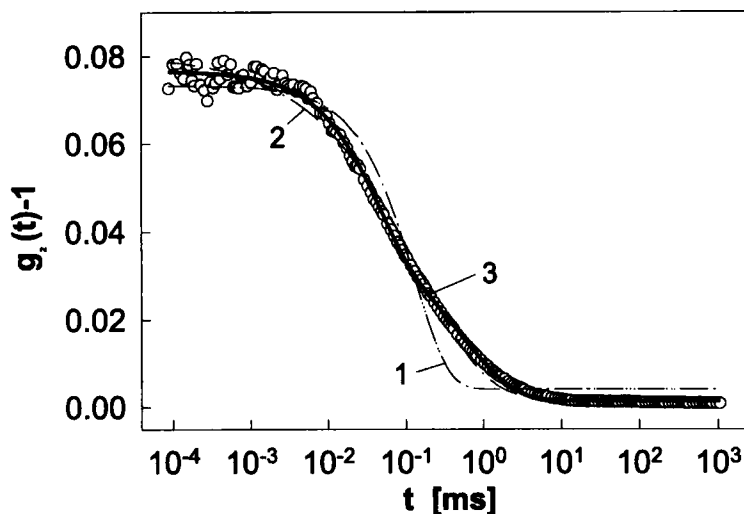


FIGURE 5 Intensity/intensity autocorrelation function for filled LC,  $T = 317.97\text{ K}$ . Open circles correspond to experimental data; lines are the result of fitting.

not be described by a single exponential decay function and the fitting line (curve 1) corresponding to this function does not follow the data. The shape of  $g_2(t)$  suggests to use a stretched exponential decay function (function 2). Indeed, if this function is used, the fitting curve (curve 2) corresponds to the experimental data reasonably well. However the fitting curve 2 slightly deviates from the experimental data in the time ranges around  $0.01\text{ ms}$  and  $1\text{ ms}$ . The best fitting (curve 3 in Fig. 1) is provided by the superposition of a single exponential and a stretched exponential decay functions. The second term (stretched exponential) dominates (this

decay is about 80 percent of the total decay).

The parameters corresponding to curve (3) in Fig. 1 are  $\tau_1 = 0.049$  ms,  $\tau_2 = 1.58$  ms, and  $\beta = 0.65$ . We assign the first (single exponential) decay to the bulk like director fluctuations. The second (stretched exponential) decay probably corresponds to the director fluctuations in the portion of LC which is bounded to the aerosil particles and belongs to a surface layer formed at particle-LC interface. The mobility of molecules could be different at different distances from the particles, which should be resulted in the appearance of a spectrum of relaxation times, what is reflected in stretched exponential decay function. Additionally, the viscosity of LC in the surface layers should be greater than the bulk viscosity, and the second process is slower than the first, the bulk-like one. In this temperature range (274 K - 335 K), both relaxation times increase with decreasing temperature. The temperature dependence of autocorrelation functions measured at different temperatures in this range are presented in Fig. 6.

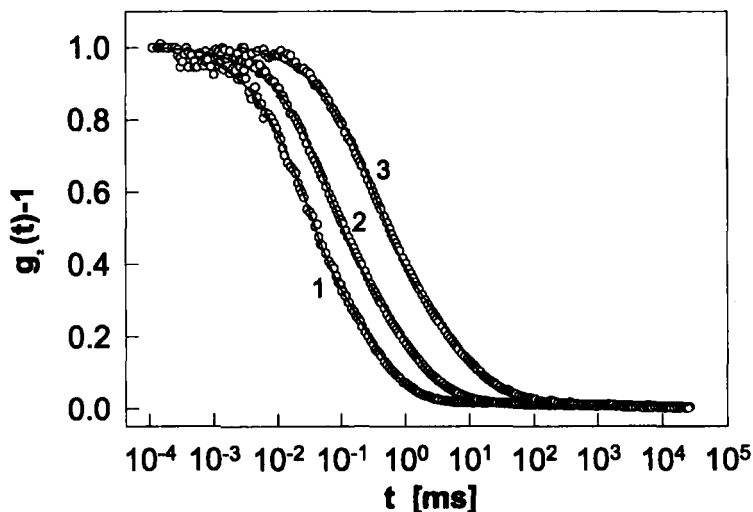


FIGURE 6 Intensity/intensity autocorrelation functions for filled LC. (1) -  $T = 337.72$  K, (2) -  $T = 305.68$  K, and (3) -  $T = 247.51$  K. Open Circles are the experimental data; lines present the result of fitting.



The parameters describing these data are: curve (1) -  $\tau_1 = 0.03$  ms,  $\tau_2 = 0.70$  ms, and  $\beta = 0.7$ ; curve (2) -  $\tau_1 = 0.07$  ms,  $\tau_2 = 2.65$  ms, and  $\beta = 0.54$ ; curve (3) -  $\tau_1 = 0.36$  ms,  $\tau_2 = 15.0$  ms, and  $\beta = 0.46$ .

The stretched exponential behavior of the second process is accompanied by a glass-like temperature dependence of corresponding relaxation time as it usually takes place in glass forming fluids<sup>[13]</sup>. This is illustrated by Fig. 7, which presents Vogel-Fulcher plot, according to the formula (6). The parameters describing this dependence are  $\tau_0 = 1.5 \cdot 10^{-5}$  s,

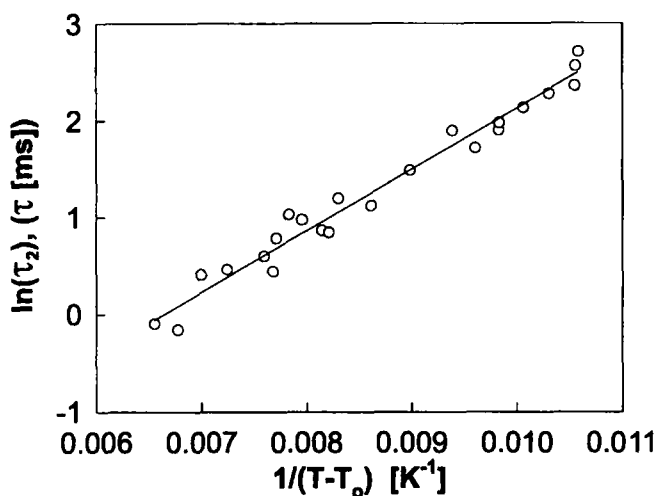


FIGURE 7 The relaxation time as function of inverse temperature in FN.

$B = 630$  K and  $T_0 = 180$  K. The temperature dependencies of  $g_2(t)$  qualitatively change in the temperature range  $T > 340$  K. In this temperature range, both relaxation times decrease when the temperature is lowered from 359 K to 335 K and an additional slow decay at  $t > 10$  ms becomes evident. This is illustrated in Fig. 8. The picture is opposite to the dependence in Fig. 6. In this temperature range, the shape of  $g_2(t)$  for filled LC (curves 1 and 2) is similar to that for 5CB confined in 100 nm random pores. The rise of relaxation times with increasing temperature could be

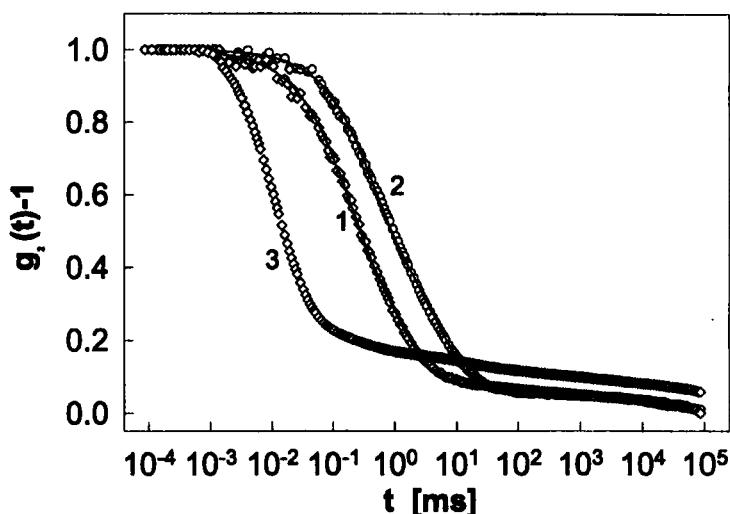


FIGURE 8 Intensity/intensity autocorrelation functions for FN (1,2) and for NLC confined in 100 nm random pores (3) LC. (1) -  $T = 344.10$  K, (2) -  $T = 374.58$  K, (3) -  $T = 294.77$  K. Open circles show the experimental data; lines are the result of fitting.

observed for a bulk LC for modes related to the director fluctuations. In this case, the temperature dependencies of the viscosity and the elastic constant are different in the vicinity of nematic - isotropic phase transition (of course in the nematic phase). An elastic constant decreases much faster than a viscosity if the temperature approaches the phase transition point, and the rise of the relaxation time of the director fluctuations should be observed.

These correlation functions are complicated. Probably, one additional process which is frozen at low temperatures, such as, for example, a rotation of LC domains as a whole, contributes to the observed  $g_2(t)$  at higher temperatures. The temperature dependencies of relaxation times of director fluctuations of bulk and filled LC are presented in Fig. 9. The relaxation times of filled LC are greater than that of the bulk LC, and they have different temperature dependence. It should be mentioned that the rise of director fluctuations' relaxation times with increasing temper-

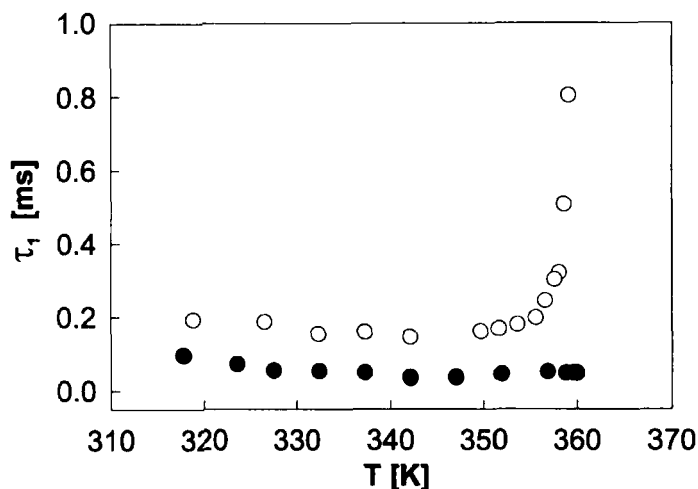


FIGURE 9 Temperature dependence of relaxation times of director fluctuations. Filled E48 - open circles, bulk pure E48 - closed circles.

ature could be observed for a bulk LC for modes related to the director fluctuations, however, for this particular LC E48 this kind of behavior is not the case.

The increase of the director fluctuations relaxation time at the temperatures close to nematic- isotropic phase transition, is mostly related to the destabilizing of the network, and therefore drastically reducing the elastic constants. Compared to covalent bonds the energy of hydrogen bonds stabilizing the network is relatively low so that they can be unlocked by mechanical interaction and are subsequently available for the formation of new bonds thus fixing a new spatial arrangement of the aggregates. This can be seen in analogy to the hydrogen bonds in organic matter. The reorientation of the director in an external electric field then can lead to a rearrangement. During this process hydrogen bonds may be broken, and new ones formed with the surface orientation adjusted to the aligned director. Investigations of this effect have shown a strong temperature dependence of the stability of the network and its elastic properties<sup>[21]</sup>. For the given dispersion of around 2.8%Vol. of Aerosil R976 in the liquid crys-

tal E48 a almost complete destabilizing of the network has been observed when approaching the nematic-isotropic phase transition temperature.

## CONCLUSION

From static light scattering experiments we obtained that nematic-isotropic phase transition temperature of LC is depressed in 100 nm random, 20 nm and 200 nm cylindrical pores compared to the bulk value. This phase transition was not detected at all in 10 nm random pores. The temperature dependence of  $I_{sc}$  in isotropic phase of confined LC is different from that in the bulk. In pores,  $I_{sc}$  does not obey the Landau theory and is almost independent of temperature in the temperature range corresponding to the isotropic phase.

The photon correlation experiments show significant changes in physical properties of both filled and confined LC and suggest that there is some evidence for glass-like dynamical behavior, although bulk liquid crystals do not have glassy properties neither in anisotropic nor in isotropic phases. We found that even about 20°C below bulk crystallization temperature the relaxational processes in confined LC were not frozen. The relaxational processes in filled and confined LC are essentially non single exponential. Slow relaxational process which does not exist in bulk LC and a broad spectrum of relaxation times ( $10^{-8} - 10$ )s appear for LC confined in random and in cylindrical pores.

Since both the slow relaxational process which does not exist in the bulk LC and the broad spectrum of relaxation times appear not only for LC in random pores but in cylindrical pores and FN as well, we suggest that differences in dynamical behavior of confined LC from that in the bulk are mainly due to the existence of the interface.

## Acknowledgments

This work was supported by US Air Force grant F49620-95-1-0520 and NSF grant OSR- 9452893.

## References

- [1.] P.S. Drzaic, *Liquid Crystal Dispersions*, (World Scientific, Singapore, 1995)
- [2.] *Liquid Crystals in Complex Geometries*, edited by G.P. Crawford and S. Zumer (Taylor and Francis, London, 1996)
- [3.] D. Finotello and J. Iannacchione, *Int.Journ.Mod.Phys.*, **B9**, 109 (1995)
- [4.] G.P. Crawford and S. Zumer, *Int. Journ. Mod. Phys.*, **B9**, 331 (1995)
- [5.] F.M. Aliev, in *Access in Nanoporous Materials*, edited by T.J. Pinnavaia and M.F. Thorpe, (Plenum Press, New York, 1995), pp. 335-354
- [6.] X-l. Wu, W.I. Goldberg, M.X. Liu, and J.Z Xue, *Phys. Rev. Lett.*, **69** 470, (1992)
- [7.] W.I. Goldberg, F.M. Aliev, X-l. Wu, *Physica A* **213**, 61 (1995)
- [8.] T. Bellini, N.A. Clark, D.W. Schaefer, *Phys. Rev. Lett.*, **74**, 2740 (1995)
- [9.] F.M. Aliev and V.V. Nadtotchi in: *Disordered Materials and Interfaces*, edited by H.Z. Cummins, D.J. Durian, D.L. Johnson, and H.E. Stanley, *Mater. Res. Soc. Proc.*, (Pittsburgh, PA, 1996), **407**, p. 125-130.
- [10.] A. Mertelj, L. Spindler, and M. Copic, *Phys. Rev. E*, **56**, 549 (1997)
- [11.] M. Kreuzer, R. Eidenschink, T. Tschudi, *Mol. Cryst. Liq. Cryst.*, **223**, 219 (1992).
- [12.] M. Kreuzer, T. Tschudi, W.H. de Jeu, R. Eidenschink, *Appl. Phys. Lett.* **62**, 1712 (1993)
- [13.] M. Kreuzer and R. Eidenschink in *Liquid crystals in complex geometries*, edited by G.P. Crawford and S. Zumer (Taylor & Francis, London, 1996), Chap. 15, p. 307
- [14.] P.G. de Gennes and J. Prost, *The Physics of Liquid Crystals*, second ed., (Clarendon Press, Oxford 1993)
- [15.] J.C. Phillips, *Rep. Prog. Phys.*, **59**, 1133 (1996)
- [16.] D. Huse, *Phys. Rev. B.*, **36**, 5383 (1987)
- [17.] M. Randieria, J. Sethna, and R.G. Palmer, *Phys. Rev. Lett.*, **54**, 1321 (1985)
- [18.] Michael, G., Ferch, H., *Grundlagen und Anwendungen von AEROSIL*, Schriftenreihe Pigmente Heft 11, 5th Edn, Frankfurt: Degussa AG (1993)
- [19.] M. Bittner, M. Kreuzer, *Mol. Cryst. Liq. Cryst.*, **282**, 373 (1996)
- [20.] T. Vogeler, M. Kreuzer, T. Tschudi, F. Simoni, *Mol. Cryst. Liq. Cryst.*, **282**, 419 (1996)
- [21.] M. Kreuzer, T. Tschudi, New materials for Optical Data Storage and High Information Content Displays, in 'Laser in Engineering', Ed. W. Waidelich, Springer Verlag Berlin 1994, pp. 804-806, ISBN 3-540-57444-1